ORIGINAL ARTICLE

Early Glaucoma Discrimination Index

Hend Safwat[1], Elaraby Nassar[2], Afaf Rashwan[3]

Abstract

Purpose: To develop a new structural algorithm derived from optical coherence tomography (OCT) retinal nerve fiber layer (RNFL) thickness and asymmetry and validate it as a discriminate among normal, suspect, and early primary open-angle glaucoma (POAG).

Study design: A case-controlled observational clinical study.

Materials and methods: In total, 150 subjects (299 eyes) were selected, 61 normal, 46 suspect, and 43 early glaucoma, from Al-Azhar University Hospitals. They were in fifth decade and free from any ocular or systemic diseases affecting the retinal nerve fiber layer. They were investigated by two consecutive perimetry (1 month apart), and three scans of circumpapillary retinal nerve fiber layer (cpRNFL) by using Nidek spectral domain (SD)-OCT 3000 Lite. The cpRNFL thickness (cpRNFLT) and inter-eye asymmetry parameters were analyzed among the three groups. Then some selected parameters were selected and analyzed using a binary logistic regression analysis for developing the new algorithm. The new algorithm was tested for the best fitting, accuracy, and diagnostic ability among the three groups and was validated in the suspect group.

Results: The new algorithm model [early glaucoma discrimination index (EGDI)] works well with only four variables; whole cpRNFLT, inferior quadrant cpRNFLT, inferotemporal clock hour (CH) cpRNFLT, and absolute inter-eye inferior quadrants asymmetry. The highest area under the curve (AUC) obtained from the EGDI among the three groups was 0.854. The validation analysis in the suspect group revealed a higher diagnostic ability in discrimination of early glaucoma with AUC of 0.989 (0.976–1.003).

Conclusion: The EGDI showed better diagnostic ability for diagnosis of glaucoma in the pre-perimetric stage. The new OCT algorithm is simple and can be run in any SD-OCT device without dependence on normative data.

Keywords: Glaucoma, Optical coherence tomography, Retinal nerve fiber layer.

Journal of Current Glaucoma Practice (2020): 10.5005/jp-journals-10078-1271

Introduction

About 50% of all glaucoma cases are undiagnosed in the developed countries, while this figure rises to 90% in the developing ones.[1] Glaucoma can remain asymptomatic until later stages. Thus, the percentage of affected individuals could be higher than recorded.[2] Glaucoma is primarily an optic neuropathy. Hence, optic nerve's functional and structural evaluation is the cornerstone of glaucoma diagnosis. Structural evaluation has evolved from clinical examination and diagramming of optic nerve head (ONH) to the current computerized methods. Optical coherence tomography (OCT) is a noncontact, noninvasive digital imaging technique of layers of the retina by analyzing interference patterns of reflected laser beam.[3] Spectral domain (SD)-OCT can detect the light echoes simultaneously by measuring the interference spectrum, using an interferometer with a high-speed spectrometer. This technique achieves scan rates of 20,000 to 52,000 A-scans per second and a resolution of 5–7 µm in tissue, mimicking an *in vivo* "optical biopsy" of the retina.[4,5] Spectral domain-OCT cannot be considered as a single diagnostic tool in glaucoma because of bias in both its normative database (reference database) and its reproducibility of circumpapillary retinal nerve fibre layer (cpRNFLT) thickness.[5] Our aim is to develop a multistructural and reproducible OCT algorithm for early glaucoma diagnosis.

Materials and Methods

We selected 150 participants (299 eyes), who visited our university hospital ophthalmic outpatient clinic in the period from May 2012 to March 2016. Al-Azhar University Ethics Committee approval has been obtained. We also adhered to the Tenets of the Declaration of Helsinki. Each participant was informed of the nature of the study, and his or her willingness to participate was documented in a written consent. All participants met the following inclusion criteria: in the fifth decade, the best corrected visual acuity 0.5 or better, +5 to −5 D sphere, astigmatism less than 3 D, and open angle on gonioscopy. The exclusion criteria were set to ensure that primary open angle glaucoma (POAG) was the cause behind changes in cpRNFLT. Hence, participants with refraction out of range of ±5 D were excluded. Similarly, participants with either ocular pathology or ONH abnormality were excluded. All participants were examined clinically by an expert examiner according to the following protocol: (1) refraction (using Topcon auto-kerato-refractometer KR-800S; Topcon Inc., Japan), (2) the best corrected visual acuity, (3) slit lamp examination, (4) intraocular pressure measurement using Goldmann's applanation tonometer, (5) gonioscopy (three-mirror Goldmann's contact lens), and (6) assessment of optic disc and retina (after dilatation of pupil) by 90-D Volk lens.

[1,3]Department of Ophthalmology, Faculty of Medicine for Girls, Al-Azhar University, Cairo, Egypt

[2]Department of Ophthalmology, Faculty of Medicine, Al-Azhar University, Cairo, Egypt

Corresponding Author: Hend Safwat, Department of Ophthalmology, Faculty of Medicine for Girls, Al-Azhar University, Cairo, Egypt, Phone: +201000504161, e-mail: doctorhend@gmail.com

How to cite this article: Safwat H, Nassar E, Rashwan A. Early Glaucoma Discrimination Index. J Curr Glaucoma Pract 2020;14(1): 16–24.

Source of support: Nil

Conflict of interest: None

Standard Automated Perimetry

Field testing was done for all participants, using two consecutive tests, 1 month apart, to avoid learning curve effect. Participants with significant field changes were tested with a third field, within 3 months, to confirm glaucomatous diagnosis. Standard automated perimetry (SAP) was done by Humphrey field analyzer II-i Series (model 745i; Crl Zeiss Meditech, Inc., Dublin, CA, USA). We used Swedish Interactive Threshold Algorithm (SITA) standard, central 24-2 threshold test. We classified the participants into three groups:

- Normal group: participants with bilateral normal eyes (clinically and functionally).
- Suspect group: POAG suspects (unilateral or bilateral ocular hypertension, suspect glaucomatous optic neuropathy, or suspect SAP) and free of any ocular or systemic diseases affecting eye RNFL.
- Glaucomatous group: early diagnosed unilateral or bilateral (mild to moderate) POAG [clinically and functionally after three consecutive perimetry (within 3 months)] and free of any ocular or systemic diseases affecting eye RNFL.

OCT Imaging

All scans were done by one operator—to avoid interoperator variability—using the same Nidek SD-OCT RS-3000 Lite device (Nidek Co., Ltd., Japan) running the NAVIS-EX software and ensured proper seating and aligning of the participant to look at the internal fixation. Then, we selected "the optic disc map"; X–Y, 6 × 6 mm square, 512 A-scans (horizontal) × 128 B-scans (vertical) in a raster fashion. Next, the ONH was centered manually and guided by the en face fundus live image before optimizing the image. After the scanning process was on, the instrument's 735-nm wavelength laser beam generated a square of data measuring 6 × 6 mm around the optic disc. The automated built-in algorithm finds the center and margin of the optic disc and extracts a B-scan in the shape of a square of 6 × 6 mm diameter using the center of the optic disc as the center of the square. Only scans with signal strength ≥7 were considered. We rejected any scans with motion artifacts, poor centration, poor focus, or missing data.

Statistical Analysis

A descriptive analysis of each parameter obtained from cpRNFL printout was performed. The mean, standard deviation (SD), and 95% confidence interval (CI), among the three groups, were analyzed. Next, the descriptive analysis for the absolute inter-eye asymmetrical parameters was also evaluated. The statistical significance of difference among the three groups was done by one-way analysis of variance followed by Bonferroni *post hoc* test. Levels of *p* less than 0.05 were considered statistically significant. To assess the ability of thickness and asymmetrical parameters in all cpRNFL sectors to discriminate eyes with glaucoma or suspect from normal eyes, the receiver operating characteristic (ROC) curve was calculated for each measurement. This test depends on the absence or presence of the disease. We differentiated between the members of the suspect group according to the OCT parameters. We classified them as normal if their OCT parameters were normal and diseased if their OCT parameters were abnormal. An area under the curve (AUC) of 1.0 indicates that the test can differentiate between the presence or absence of the condition, whereas an AUC of 0.5 indicates a completely worthless test. The cutoff points of the best diagnostic cpRNFLT and asymmetrical parameters were calculated with the Youden index (the highest sensitivity/specificity balance). A binary logistic regression analysis was performed to calculate a linear discrimination function (LDF) designed by combining cpRNFL parameters. The goal is to differentiate glaucoma from normal participants. The predicted dependent variable was glaucoma presence, and the independent variables were whole, inferior quadrant, and inferotemporal CH of cpRNFLT and inter-eye inferior quadrant asymmetry. The relative importance of each independent variable was evaluated by Wald method. Then, the LDF [or early glaucoma discrimination index (EGDI)] score was obtained by taking a weighted sum of the predictor variables. A validation analysis was performed in the suspect group. Diagnostic ability by using ROC test for the EGDI was performed. The test was performed using SPSS for Windows, version 12.0.1 (SPSS, Inc., Chicago, IL).

Results

The number of participants was 61 (122 eyes) in the normal group, 46 (92 eyes) in the suspect group, and 43 (85 eyes) in the diseased group. One eye from glaucomatous group was excluded because of high myopia. Participants aged 44.93 ± 3.38 years in the normal, 45 ± 3 years in the suspect, and 46 ± 3 years in the glaucomatous group. The whole cpRNFLT was 107.87 ± 8.35 µm in the normal, 103.08 ± 12.50 µm in the suspect, and 98.63 ± 12.22 µm in the glaucomatous group. The inferior quadrant cpRNFLT was 140.15 ± 15.39 µm in the normal, 130.12 ± 17.96 µm in the suspect, and 121.40 ± 19.92 µm in the glaucomatous group (Table 1). The inter-eye asymmetries in cpRNFLTs among the three groups and their diagnostic accuracy are detailed in Tables 2 and 3. The parameters that showed significant changes among the three groups ($p < 0.05$) were inter-eye inferior quadrant, superior quadrant, CH 7/5, and CH 10/2. The best parameters which could differentiate the normal from the suspect were inferior, whole, and inferotemporal RNFL thickness (AUCs range: 0.836–0.742) (Table 3 and Fig. 1). The cutoff values were as following: inferior: 129.5 µm, whole: 103.8 µm, and inferotemporal: 130.5 µm. The best sensitivity at 80% specificity came from inferior cpRNFLT (67.3%). The best diagnostic value from inter-eye asymmetrical parameters was inferior quadrant asymmetry (60.7%), with cutoff point 16.49 µm. From the binary logistic regression analysis, our derived equation was

$$\text{EGDI} = 14.057 - 0.065 \times \text{whole cpRNFLT} - 0.052 \times \text{inferior quadrant cpRNFLT} - 0.012 \times \text{inferotemporal CHcpRNFLT} + 0.046 \times \text{absolute inter-eye inferior quadrants asymmetry}$$

Fitting of our model was excellent (Table 4). The Nagelkerke R^2 for the model was good (0.467). The Omnibus test for model fitting has revealed chi-square value of 126.610 with high significance ($p = 0.000$). The significance from Hosmer and Lemeshow test was excellent (0.138). The highest AUC obtained from the EGDI among the three groups was 0.854 (95% CI: 0.811–0.897) (Fig. 1). Our EGDI showed the cutoff point ≥−0.695, with the highest sensitivity–specificity. Our EGDI is 69.5 and 55% sensitive at 80 and 95% specificity, respectively, with 17.1% (61/264) misclassification rate. The LDF misclassified 21 normal participants as having glaucoma and 40 glaucoma participants as normal. While validation analysis in the suspect group revealed higher diagnostic ability in discriminating early glaucoma, with AUC: 0.989 (95% CI: 0.976–1.003). The sensitivities were 100 and 93.5% at 80 and 95% specificities, respectively. The diagnostic ability of our algorithm in the suspect group is more illustrated by clinical cases in Figures 2 to 4.

Table 1: OCT cpRNFLTs in three groups

cpRNFLT	*Normal MD ± SD (95% CI)*	*Suspect MD ± SD (95% CI)*	*Glaucoma MD ± SD (95% CI)*	*p value*	*F*	*Normal vs suspect*	*Normal vs glaucoma*	*Suspect vs glaucoma*
Whole	107.87 ± 8.35 (106.38–109.37)	103.08 ± 12.50 (100.49–105.67)	98.63 ± 12.22 (95.92–101.33)	<0.000	17.86	<0.005	<0.0001	<0.05
Temporal quadrant	69.31 ± 9.72 (67.56–71.05)	69.03 ± 12.49 (66.44–71.62)	67.58 ± 13.71 (64.55–70.62)	0.574	0.556	0.984	0.566	0.702
Superior quadrant	129.40 ± 15.10 (126.69–132.11)	126.59 ± 21.54 (122.13–131.05)	120.04 ± 19.44 (115.58–125.13)	0.005	5.485	0.538	<0.005	0.084
Nasal quadrant	88.70 ± 12.72 (86.42–90.98)	83.76 ± 16.28 (80.38–87.13)	81.74 ± 15.24 (78.37–85.11)	<0.005	6.21	<0.05	<0.005	0.638
Inferior quadrant	140.15 ± 15.39 (137.39–142.90)	130.12 ± 17.96 (126.40–133.84)	121.40 ± 19.92 (116.99–125.80)	<0.000	28.48	<0.000	<0.000	<0.005
CH 2 (OS)	81.56 ± 14.1 (77.95–85.18)	77.18 ± 17.54 (71.97–82.39)	75.62 ± 15.22 (70.81–80.43)	0.132	2.05	0.321	0.145	0.888
CH 10 (OD)	82.55 ± 12.30 (79.40–85.70)	79.46 ± 15.2 (74.93–83.93)	78.91 ± 17.11 (73.44–84.39)	0.392	0.942	0.529	0.444	0.984
CH 5 (OS)	134.62 ± 26.39 (127.86–141.38)	131.26 ± 28.14 (122.90–139.61)	118.50 ± 33.41 (107.95–129.05)	<0.05	3.967	0.823	<0.05	0.105
CH 7 (OD)	140.38 ± 22.10 (134.72–146.04)	132.86 ± 31.43 (123.53–142.20)	126.03 ± 22.09 (118.96–133.09)	<0.05	3.944	0.286	<0.05	0.429

MD, mean deviation; CH, clock hour; cpRNFL, circumpapillary retinal nerve fiber layer; $p < 0.05$ is significant.

Table 2: The absolute inter-eye cpRNFL asymmetries in three groups

Inter-eye asymmetry	*Normal (n = 61) (95% CI)*	*Suspect (n = 46) (95% CI)*	*Glaucoma (n = 42) (95% CI)*	*p value*	*F*	*Normal vs suspect*	*Normal vs glaucoma*	*Suspect vs glaucoma*
Superior quadrant	9.31 ± 8.04 (7.25–11.37)	10.43 ± 8.23 (7.89–12.88)	14.35 ± 11.72 (10.59–18.10)	<0.05	3.723	0.81	<0.05	0.126
Inferior quadrant	8.07 ± 8.59 (5.87–10.27)	10.49 ± 9.43 (7.69–13.29)	16.49 ± 18.27 (10.64–22.33)	0.004	5.827	0.57	0.003	0.063
Nasal quadrant	10.62 ± 9.30 (8.23–13.06)	9.17 ± 10.16 (6.15–12.19)	8.88 ± 8.73 (6.08–11.67)	0.6	0.513	0.712	0.637	0.989
Temporal quadrant	8.74 ± 9.77 (6.23–11.24)	10.19 ± 10.68 (7.02–13.36)	12.10 ± 12.74 (8.03–16.18)	0.32	1.147	0.775	0.288	0.698
Whole	4.52 ± 4.01 (3.49–5.55)	6.03 ± 6.83 (4.00–8.06)	7.65 ± 9.87 (4.49–10.80)	0.086	2.496	0.503	0.071	0.528
Inferotemporal CH	16.62 ± 13.11 (13.26–19.98)	18.20 ± 12.02 (14.63–21.77)	27.14 ± 21.28 (20.33–33.94)	0.003	6.021	0.86	0.003	<0.05
Superotemporal CH	10.70 ± 7.38 (8.84–12.62)	13.39 ± 11.03 (10.12–16.67)	16.15 ± 12.7 (12.09–20.22)	<0.05	3.446	0.378	<0.05	0.426

CI, confidence interval; *n*, number; CH, clock hour; cpRNFL, circumpapillary retinal nerve fiber layer; $p < 0.05$ is significant

Discussion

The reproducibility measurements should be settled before enrolling any new diagnostic device.[6] This is performed via testing the accuracy and reproducibility of cpRNFLT measurements. Numerous studies had been performed on RTVue,[7–9] Cirrus,[10–12] Spectralis,[13–15] and Nidek OCT devices.[16–18] The thickest value in cpRNFL quadrants was of inferior, followed by superior, nasal, and finally temporal, obeying the "inferior-superior-nasal-temporal (ISNT)" rule. This is reported by many authors.[19–24] However, few reviews found that the superior quadrant is the thickest (against to the "ISNT" rule).[25,26] Schuman et al.,[19] Bowd et al.,[27] and Liu et al.[28] reported that the nasal quadrant was thinner than the temporal quadrant. However, we found that the temporal RNFL thickness was thinner than the nasal ($p = 0.001$). The photographic and histological data from early research support our finding.[20–31] Hong believed that the thinner nasal RNFL in East Asians may be due to the higher prevalence of myopia in them and temporal shift in macula.[32] We believe that the differences in published studies' results are due to segmentation algorithms, difference in criteria of selection of participants, ethnicity, stages of glaucoma, and different operators. We noticed that most of the published studies in the literature do not consider the effect of age. Most studies have found a significant loss in nerve fiber layer attributed to aging that ranges from 0.15 to 0.56 µm/year.[33] Budenz et al.,[20] Bendschneider et al.,[21] and Alasil et al.[34] reported a decline of 1.5 to 2 µm/decade in OCT cpRNFLT. Consequently, we believe that the choice of the fifth decade among our study groups gives our results a further strength.

We found the whole and inferior quadrant cpRNFLTs have changed significantly among the three groups ($p < 0.0001$). The power of inferior quadrant thickness as a diagnostic parameter is due to its resistance to age changes. The highest AUC as a

Table 3: The ROC curve for cpRNFLT and asymmetrical parameters

Parameters	*AUC (95% CI)*	*p value*	*Sensitivity at 80% specificity (%)*
Whole cpRNFL	0.803 (0.748–0.857)	0.000	63.5
Temporal cpRNFL	0.625 (0.577–0.727)	0.000	47.4
Superior cpRNFL	0.677 (0.608–0.747)	0.000	39.4
Nasal cpRNFL	0.665 (0.595–0.735)	0.000	39
Inferior cpRNFL	0.836 (0.787–0.886)	0.000	67.3
Inferotemporal CH cpRNFL	0.742 (0.679–0.804)	0.000	53.5
Superotemporal CH cpRNFL	0.686 (0.616–0.756)	0.000	50.5
Inter-eye inferior quadrant asymmetry[a]	0.752 (0.664–0.839)	0.000	60.7
Inter-eye superior quadrant asymmetry[a]	0.770 (0.690–0.850)	0.000	57.9
Inter-eye 7–5 CH asymmetry[a]	0.746 (0.663–0.830)	0.000	49.2
Inter-eye 10-2 CH asymmetry[a]	0.746 (0.663–0.830)	0.000	49.2

AUC, area under curve; a, absolute; CH, clock hour; cpRNFL, circumpapillary retinal nerve fiber layer; $p < 0.05$ is significant

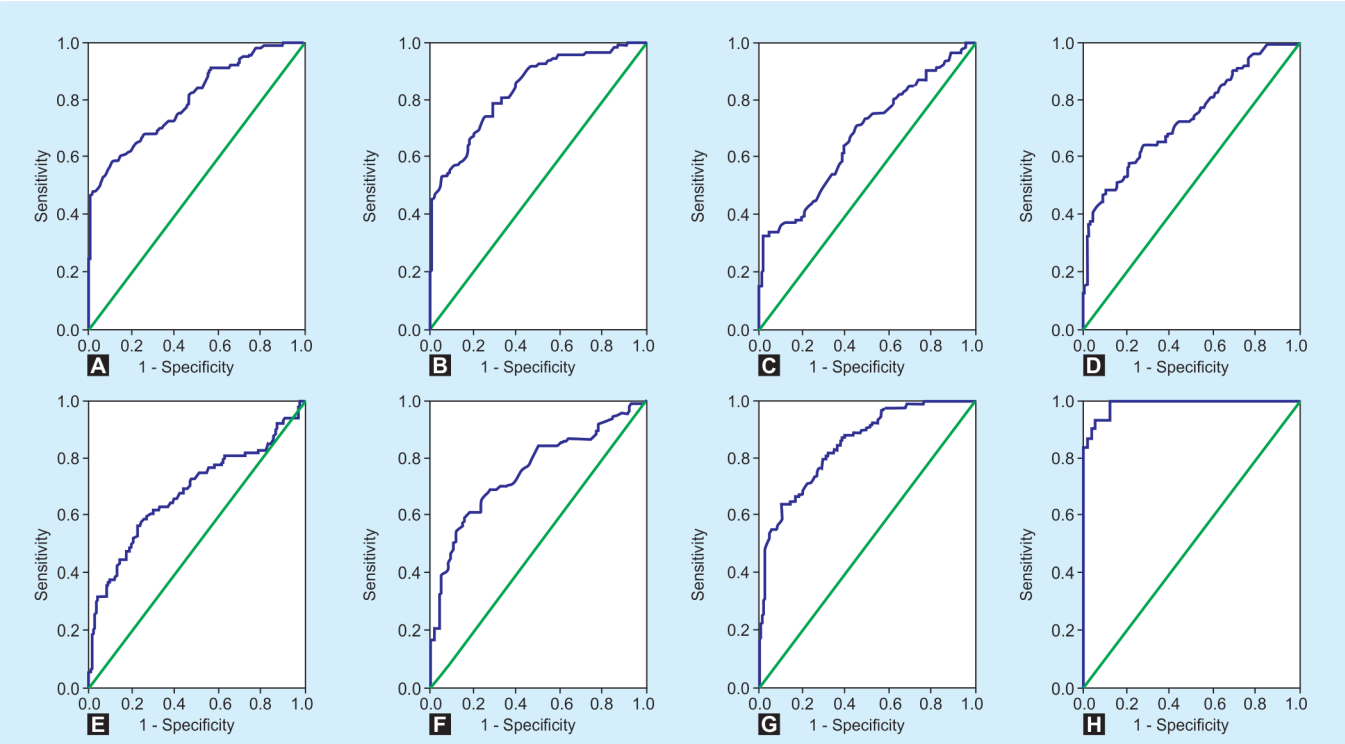

Figs 1A to H: The area under curve for: (A) Whole circumpapillary retinal nerve fiber layer (cpRNFL) (0.80); (B) Inferior quadrant cpRNFL (0.83); (C) Superior quadrant cpRNFL (0.67); (D) Inferotemporal clock hour cpRNFL (0.74); (E) Superotemporal clock hour cpRNFL (0.68); (F) Inter-eye inferior quadrants asymmetry (0.75); (G) Early glaucoma discrimination index (EGDI) algorithm among three groups (0.85); (H) EGDI algorithm in the validation group (0.98)

Table 4: The fitting tests for our model (EGDI)

	(1) Omnibus tests of model coefficients			*(2) Model summary*			*(3) Hosmer and Lemeshow test*		
Step 1	*Chi-square*	*df*	*Significance*	*–2 log likelihood*	*Cox and Snell R^2*	*Nagelkerke R^2*	*Chi-square*	*df*	*Significance*
Step	126.610	4	0.000						
Block	126.610	4	0.000						
Model	126.610	4	0.000	263.147	0.350	0.476	12.316	8	0.138

EGDI, early glaucoma discrimination index; $p < 0.05$ is significant in Omnibus test; $p > 0.05$ is significant in Hosmer and Lemeshow test

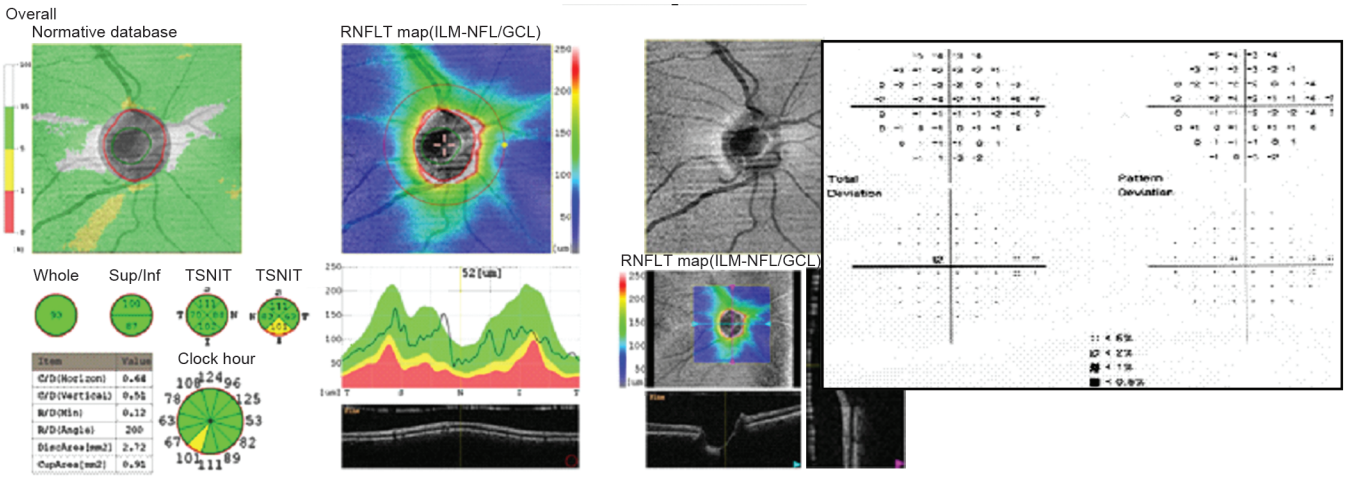

Fig. 2: Suspect glaucomatous optic neuropathy with normal perimetry. The optical coherence tomography circumpapillary retinal nerve fiber layer data: whole = 93, inferior quadrant = 102, inferotemporal clock hour = 101, and absolute inter-eye inferior quadrants asymmetry = 1. With applying our equation, the suspect early glaucoma discrimination index score = 1.542 (>−0.695), ruling in glaucomatous diagnosis

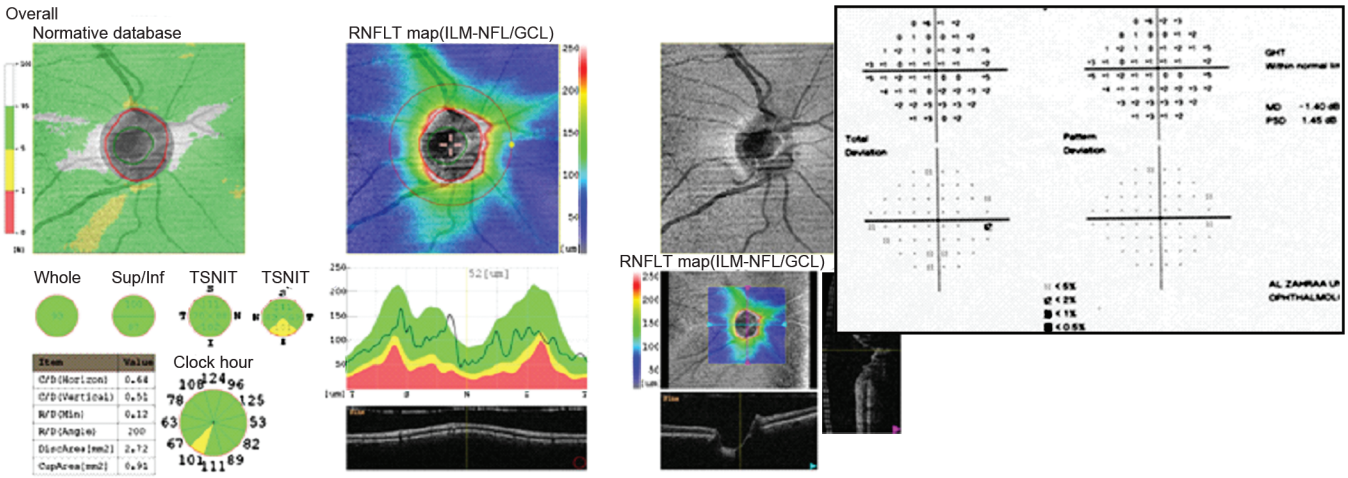

Fig. 3: Suspect glaucomatous optic neuropathy with normal perimetry. The optical coherence tomography circumpapillary retinal nerve fiber layer data: whole = 105, inferior quadrant = 126, inferotemporal clock hour = 97, and absolute inter-eye inferior quadrants asymmetry = 2. With applying our equation, the suspect early glaucoma discrimination index score = −0.392 (>−0.695), ruling in glaucomatous diagnosis

diagnostic tool for early and pre-perimetric glaucoma was inferior (0.83) and then the whole cpRNFLT (0.80). This is reported in the literature but with higher range of AUC areas. The lower diagnostic ability of RNFL thickness in nasal and temporal areas may be explained by the relatively lower amount of RNFL loss in early glaucoma. Sehi et al. found the parameters with the best performance as follows: the inferior (0.94), average (0.88), and superior (0.80) quadrant thickness.[35] Budenz et al. found that AUCs of inferior, total, and superior RNFL thickness were 0.97, 0.97, and 0.95, respectively.[36] Bowd et al. found that AUC of inferior thickness was 0.91.[37] Hwang and Kim reported higher AUC for inferior quadrant (0.986) in discriminating of the normal from the mild glaucomatous patients, while the whole cpRNFLT worked better in other stages of glaucoma.[38] Leung et al. and Park et al. found that the largest AUC for all parameters was the total cpRNFLT.[39,40] However, Leite reported the largest AUCs for superior and total cpRNFLT.[41] Mwanza et al. reported 0.89 and 0.91 AUCs for all parameters in detecting the normal from the mild glaucomatous eye.[42]

In our opinion, the higher AUCs of previous works compared with our study results are not true real clinical difference. Many factors should be taken into consideration. The higher numbers of the normal (control) group compared with the diseased group as in our study increase the chance of more false-negatives that decrease the sensitivity. Most of the previous works used glaucomatous group in an advanced or a moderate state which affects the statistical outcomes. The presence of a suspect group in our study makes the changes between the three groups appearing small during any statistical analysis activity. Also, ROC curves are applied in an "all or none" fashion. Each participant must be labeled either normal or diseased. We noticed that many works group the suspects with glaucomatous patients as one group which elevates the values of AUCs. Instead, we labeled the suspects as diseased (if OCT revealed structural defect) or as normal (if OCT revealed

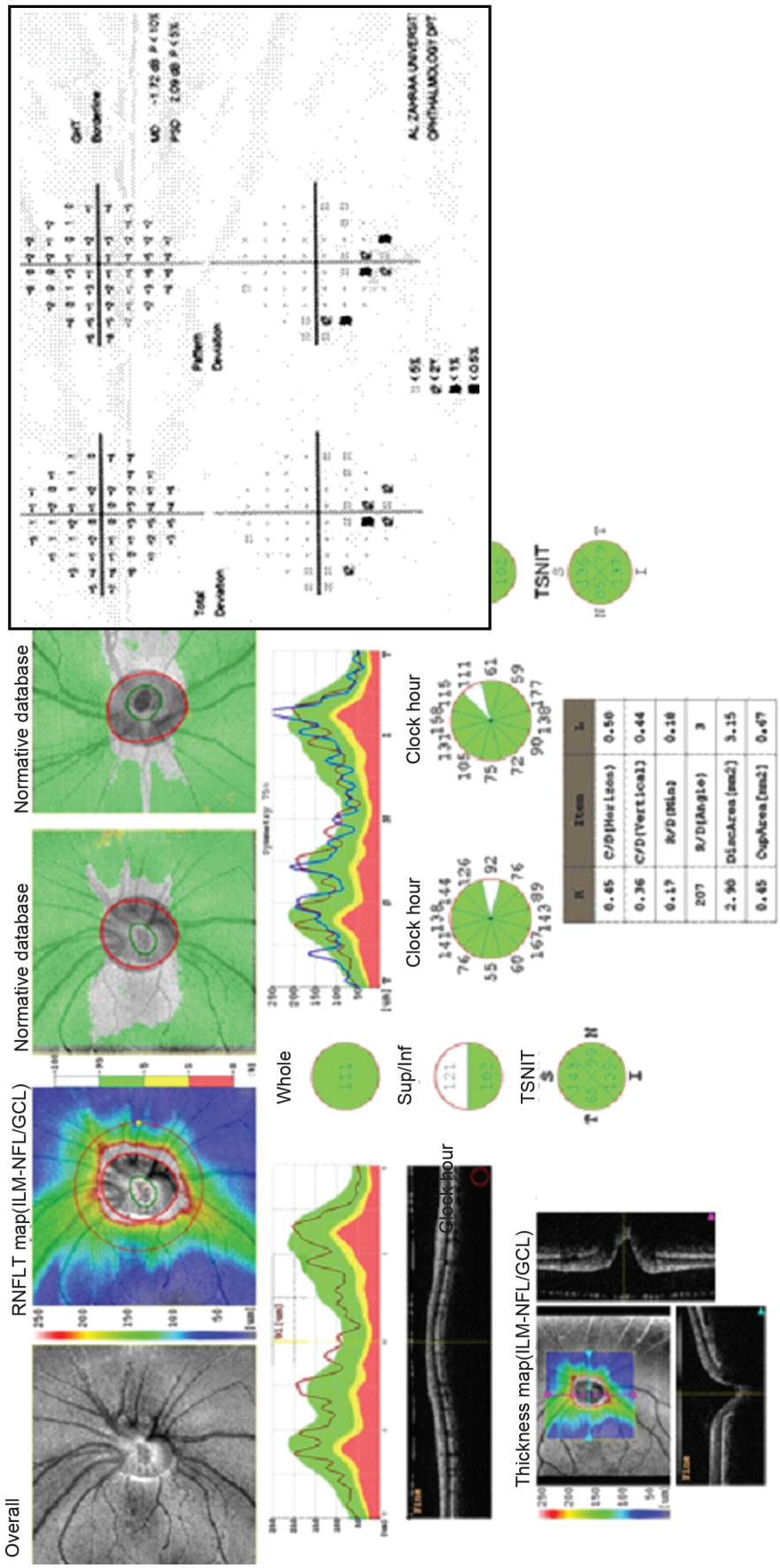

Fig. 4: Case of ocular hypertension and suspect perimetry. The optical coherence tomography circumpapillary retinal nerve fiber layer data: whole = 111, inferior quadrant = 135, inferotemporal clock hour = 167, and absolute inter-eye inferior quadrants asymmetry = 2. With applying our equation, the suspect early glaucoma discrimination index score = −2.09 (<−0.695), ruling out glaucomatous diagnosis

no structural defect). We believe that a control group with some diagnostic uncertainty mimics real-life clinical state than a purely normal control group.

The inferotemporal region of the ONH is first affected because of the glaucomatous preferential loss. This is consistent with a higher incidence of upper nasal step in early glaucomatous perimetry.[43–45] Leung et al.[46] and Xu et al.[47] supported in their studies the preferential glaucomatous affection of inferotemporal sector in early glaucoma which expands to take inferior quadrant cpRNFL in moderate glaucoma.

C:D ratio asymmetry and inter-eye cpRNFLT asymmetry are analog.[48] The inter-ocular differences in RNFL thickness in healthy eyes are due to density of retinal ganglion cell (RGC) axons and the contribution of other structures such as blood vessels.[49,50] We found the valuable inter-eye asymmetry parameters ($p < 0.05$) between the three groups as follows: inferior and superior quadrants, 7/5, and 10/2 CHs. We agree with Sullivan-Mee et al.'s inter-eye asymmetry parameters.[51] Park et al. found that the inter-eye temporal-superior-nasal-inferior-temporal (TSINT) graph difference more than 50 µm can detect most of RNFL defects.[52] Asrani et al. published a case presentation that concluded that inter- and intra-eye asymmetry, in the presence of normality in classic cpRNFL and macular ganglion cell complex (mGCC) thickness maps, can raise the OCT sensitivity in diagnosing pre-perimetric as well as early glaucoma.[53] For inter-eye parameters, the best sensitivity was elicited by inferior quadrant (60.7%). We agree in some values with Sullivan-Mee et al. and Khanal studies.[51,54] The intra-eye and inter-eye asymmetries are more precise in diagnosis than the thickness values for these reasons: no fixed circular scan (and ONH size bias) dependence, no comparison with normative data base (and selection bias), and dependence on the personal eye as reference.[49,51,54,55]

To our knowledge, this study is the first to use only multivariate cpRNFLTs in a single LDF. Also, we used the conventional parameters reported by the OCT protocols and the new asymmetrical parameters. We developed our own LDF algorithm model for early prediction of glaucoma in the pre-perimetric stage. Our model depends on inter-eye absolute inferior quadrant asymmetry that showed the higher AUC and sensitivity among all inter-eye asymmetrical parameters. The other variables which were included in this model were chosen based on the preferential glaucoma affection and their higher AUCs. The strength of this model is executing it on the three groups including the suspects. Our EGDI elicited the higher AUC among all variables (0.811–0.897). The diagnostic ability became perfect (0.976–1.003) when the index validated in the suspect group only.

Reviewing the literature, we found some investigators who combined structural parameters with their own algorithms to enhance glaucoma diagnosis. Early investigators combined structures derived from different devices as Badala et al. [i.e., scanning laser ophthalmoscope (SLO) and scanning laser polarimetry (SLP) or SLO and OCT].[56] Medeiros et al.[57] launched their LDF (combination of selected RNFL and ONH parameters) and validated it (AUC = 0.97) in an independent population. But the validation sample was small and only of moderate and advanced glaucoma rather than early glaucoma.

Pablo et al.[58] used logistic regression and developed their own LDF which was based on ONH parameters. They reported AUC for their LDF algorithm (0.864–0.961), with 72% sensitivity at 95% specificity. Although their results share some similarity with our findings, they used time domain (TD)-OCT which has errors in ONH segmentation algorithms. TD-OCT defines the ONH margin as the endings of the retinal pigment epithelium (RPE), which may overestimate of disc margin in case of para- or peripapillary atrophy. This minimizes the accuracy of these parameters. In general, we noticed that the presence of a suspect group affects the statistical results. Previous works differentiated only the normal from the established early glaucoma which leads to higher statistical significance. In our opinion, the challenge in using OCT in glaucoma diagnosis is evaluating the suspect group, rather than the glaucoma patients already diagnosed via perimetry.

Sugimoto et al.[59] developed a classifier (developed via using random forest statistics), to predict the presence of visual field deterioration in glaucoma suspects Their model consisted of 237 different measurements combining OCT (ONH, cpRNFL, mRNFL, and mGCC parameters), age, gender, axial length, and laterality of the eye. They reported AUC for their algorithm (0.90). However, we used a smaller number of OCT variables (4 vs 237), making our model easier to calculate. Also, they had not a normal group with lack of a normative population to act as a reference.

Mwanza et al.[60] found LDF with 16 variables (5 RNFL, 3 ONH, and 8 mGCC), and an AUC of 0.995 with 98.6% sensitivity and 96.0% specificity. The higher result may be due to many factors in their study. They used Cirrus OCT which is able to do automatic centration on optic disc, cpRNFL segmentation done from 3D (not 2D) cube scanning, and ability to segment macular ganglion cell layer + inner plexiform layer without axons. Also, they did not study the suspect group which makes the LDF expected to report higher statistically significant results. They used exploratory factor analysis with the ability to reduce cross-loadings, which lead to decreased input parameters, and it is similar in performance to the multiple logistic regression models.

The advanced imaging for glaucoma (AIG) study has recently proposed the glaucoma structural diagnostic index (GSDI).[61] A multivariate logistic model was used to construct the GSDI. Their formula was [−0.74 × composite overall thickness + 0.70 × composite focal loss volume (FLV) + 3.37 × vertical cup disc ratio (VCDR) − 3.69]. The AUC for GSDI was 0.922, significantly better than the AUC for the best single component variable; and sensitivity was 80% at 95% specificity. The AIG study used the case:control ratio of 2:1. However, their model is simple and easy to be applied by using their equation.

Choi et al. found that using LDF from multiple OCT parameters is better than single OCT parameter in differentiating the healthy from early glaucomatous persons.[62] Their proposed LDF was 16.529 − (0.132 × superior RNFL) − (0.064 × inferior RNFL) + (0.039 × 12 o'clock RNFL) + (0.038 × 1 o'clock RNFL) + [0.084 × superior ganglion cell inner plexiform layer (GCIPL)] − (0.144 × minimum GCIPL). In the validating set, the LDF showed significantly higher AUC than the best RNFL (inferior RNFL). Their study is strengthened by using a validating test to avoid overdiagnosis by LDF. However, their study is limited by the absence of a pre-perimetric or a suspect glaucoma group.

Although our study's sample size is more or less as the similar studies' sample size, it should be continued. For more validation, it should be tested in another set of peoples, not included here, and another OCT devices with different segmentation algorithms.

Conclusion

We found that combining specific OCT cpRNFL parameters is better than depending on color-coded built-in reference database.

The inter-eye asymmetries are more reliable due to depending on within-subject reference. We hope our new glaucoma probability index will help in early diagnosis of POAG.

References

1. Broadway DC, Glaucoma: WHO has estimated that 4.5 million people are blind due to glaucoma. Available from: http://www.iapb.org/vision-2020/what-is-avoidable-blindness/glaucoma, accessed on 12 April 2016.
2. Weinreb RN, Aung T, Medeiros FA. The pathophysiology and treatment of glaucoma: a review. JAMA 2014;311(18):1901–1911. DOI: 10.1001/jama.2014.3192.
3. Meier KL, Greenfield DS, Hilmantel G, et al. Special commentary: Food and drug administration and american glaucoma society co-sponsored workshop: the validity, reliability, and usability of glaucoma imaging devices. Ophthalmology 2014;121(11):2116–2123. DOI: 10.1016/j.ophtha.2014.05.024.
4. Cheema A, Moore DB, Griffiths D. Spectral domain optical coherence tomography in glaucoma [updated 2015 Jan 27; cited 2015 Jan 27]. Available from: http://eyewiki.aao.org/Spectral_Domain_Optical_Coherence_Tomography_in_Glaucoma.
5. Adhi M, Duker JS. Optical coherence tomography – current and future applications. Curr Opin Ophthalmol 2013;24(3):213–221. DOI: 10.1097/ICU.0b013e32835f8bf8.
6. Kamppeter BA, Schubert KV, Budde WM, et al. Optical coherence tomography of the optic nerve head interindividual reproducibility. J Glaucoma 2006;15(3):248–254. DOI: 10.1097/01.ijg.0000212205.02771.b7.
7. Garas A, Vargha P, Holló G. Diagnostic accuracy of nerve fibre layer, macular thickness and optic disc measurements made with the RTVue-100 optical coherence tomograph to detect glaucoma. Eye 2011;25(1):57–65. DOI: 10.1038/eye.2010.139.
8. González-García AO, Vizzeri G, Bowd C, et al. Reproducibility of RTVue retinal nerve fiber layer thickness and optic disc measurements and agreement with stratus optical coherence tomography measurements. Am J Ophthalmol 2009;147(6):1067–1074. DOI: 10.1016/j.ajo.2008.12.032.
9. Garas A, Vargha P, Holló G. Reproducibility of retinal nerve fiber layer and macular thickness measurement with the RTVue-100 optical coherence tomograph. Ophthalmology 2010;117(4):738–746. DOI: 10.1016/j.ophtha.2009.08.039.
10. Leung CK, Cheung CY, Weinreb RN, et al. Retinal nerve fiber layer imaging with spectral-domain optical coherence tomography: a variability and diagnostic performance study. Ophthalmology 2009;116(7):1257–1263. DOI: 10.1016/j.ophtha.2009.04.013.
11. Sung KR, Kim DY, Park SB, et al. Comparison of retinal nerve fiber layer thickness measured by cirrus HD and stratus optical coherence tomography. Ophthalmology 2009;116(7):1264–1270. DOI: 10.1016/j.ophtha.2008.12.045.
12. Garcia-Martin E, Pinilla I, Idoipe M. Intra and interoperator reproducibility of retinal nerve fibre and macular thickness measurements using cirrus fourier-domain OCT. Acta Ophthalmol (Copenh) 2011;89(1):e23–e29. DOI: 10.1111/j.1755-3768.2010.02045.x.
13. Mansoori T, Viswanath K, Balakrishna N. Reproducibility of peripapillary retinal nerve fibre layer thickness measurements with spectral domain optical coherence tomography in normal and glaucomatous eyes. Br J Ophthalmol 2011;95(5):685–688. DOI: 10.1136/bjo.2010.183020.
14. Langenegger SJ, Funk J, Töteberg-Harms M. Reproducibility of retinal nerve fiber layer thickness measurements using the eye tracker and the retest function of spectralis SD-OCT in glaucomatous and healthy control eyes. Invest Ophthalmol Vis Sci 2011;52(6):3338–3344. DOI: 10.1167/iovs.10-6611.
15. Serbecic N, Beutelspacher SC, Aboul-Enein FC, et al. Reproducibility of high-resolution optical coherence tomography measurements of the nerve fibre layer with the new Heidelberg Spectralis optical coherence tomography. Br J Ophthalmol 2011;95(6):804–810. DOI: 10.1136/bjo.2010.186221.
16. Pierro L, Gagliardi M, Iuliano L, et al. Retinal nerve fiber layer thickness reproducibility using seven different OCT instruments. Ophthalmol Vis Sci 2012;53(9):5912–5920. DOI: 10.1167/iovs.11-8644.
17. Kita Y, Holló G, Kita R, et al. Differences of intrasession reproducibility of circumpapillary total retinal thickness and circumpapillary retinal nerve fiber layer thickness measurements made with the RS-3000 optical coherence tomograph. PLoS ONE 2015;10(12):e0144721. DOI: 10.1371/journal.pone.0144721.
18. K121622 510 (k) Summary about optical coherence tomography RS-3000. FDA approval letter to Nidek Co., Ltd. [published 2013 Mar 14; cited 2014 Jan 20]. Available from: https://510k.directory/clearances/K121622.
19. Schuman JS, Hee MR, Puliafito CA, et al. Quantification of retinal nerve fiber layer thickness in normal and glaucomatous eyes using optical coherence tomography (a pilot study). Arch Ophthalmol 1995;113(5):586–596. DOI: 10.1001/archopht.1995.01100050054031.
20. Budenz DL, Anderson DR, Varma R, et al. Determinants of normal retinal nerve fiber layer thickness measured by stratus OCT. Ophthalmology 2007;114(6):1046–1052. DOI: 10.1016/j.ophtha.2006.08.046.
21. Bendschneider D, Tornow RP, Horn FK, et al. Retinal nerve fiber layer thickness in normals measured by spectral domain OCT. J Glaucoma 2010;19(7):475–482. DOI: 10.1097/IJG.0b013e3181c4b0c7.
22. Leite MT, Rao HL, Weinreb RN, et al. Agreement among spectral-domain optical coherence tomography instruments for assessing retinal nerve fiber layer thickness. Am J Ophthalmol 2011;151(1):85–92. DOI: 10.1016/j.ajo.2010.06.041.
23. Buchser NM, Wollstein G, Ishikawa H, et al. Comparison of retinal nerve fiber layer thickness measurement bias and imprecision across three spectral domain optical coherence tomography devices. Invest Ophthalmol Vis Sci 2012;53(7):3742–3747. DOI: 10.1167/iovs.11-8432.
24. Agarwal P, Saini VK, Gupta S, et al. Evaluation of central macular thickness and retinal nerve fiber layer thickness using spectral domain optical coherence tomography in a tertiary care hospital. J Curr Glaucoma Pract 2014;8(2):75–81. DOI: 10.5005/jp-journals-10008-1165.
25. Ramakrishnan R, Mittal S, Ambatkar S, et al. Retinal nerve fibre layer thickness measurements in normal Indian population by optical coherence tomography. Indian J Ophthalmol 2006;54(1):11–16. DOI: 10.4103/0301-4738.21608.
26. Kanamori A, Nakamura M, Escano MFT, et al. Evaluation of the glaucomatous damage on retinal nerve fiber layer thickness measured by optical coherence tomography. Am J Ophthalmol 2003;135(4):513–520. DOI: 10.1016/s0002-9394(02)02003-2.
27. Bowd C, Weinreb RN, Williams JM, et al. The retinal nerve fiber layer thickness in ocular hypertensive, normal, and glaucomatous eyes with optical coherence tomography. Arch Ophthalmol 2000;118(1):22–26. DOI: 10.1001/archopht.118.1.22.
28. Liu X, Ling Y, Luo R, et al. Optical coherence tomography in measuring retinal nerve fiber layer thickness in normal subjects and patients with open-angle glaucoma. Chin Med J 2001;114(5):524–529.
29. Frenkel S, Morgan JE, Blumenthal EZ. Histological measurement of retinal nerve fibre layer thickness. Eye 2005;19(5):491–498. DOI: 10.1038/sj.eye.6701569.
30. Harizman N, Oliveira C, Chiang A, et al. The ISNT rule and differentiation of normal from glaucomatous eyes. Arch Ophthalmol 2006;124(11):1579–1583. DOI: 10.1001/archopht.124.11.1579.
31. Lundmark PO, Skjöld GB, Nævdal PA, et al. Use of ISNT rule for optic disc evaluation in 40 to 79 year old patients seen in optometric practice. SJOVS 2010;3(1):16–22. DOI: 10.5384/SJOVS.vol3i1p16.
32. Hong SW, Ahn MD, Kang SH, et al. Analysis of peripapillary retinal nerve fiber distribution in normal young adults. Invest Ophthalmol Vis Sci 2010;51(7):3515–3523. DOI: 10.1167/iovs.09-4888.
33. Zhang X, Francis BA, Dastiridou A, et al. Longitudinal and cross-sectional analyses of age effects on retinal nerve fiber layer and ganglion cell complex thickness by Fourier-domain OCT.

Translational Vision Science & Technology 2016;5(2):1–6. DOI: 10.1167/tvst.5.2.1.
34. Alasil T, Wang K, Keane PA, et al. Analysis of normal retinal nerve fiber layer thickness by age, sex, and race using spectral domain optical coherence tomography. J Glaucoma 2013;22(7):532–541. DOI: 10.1097/IJG.0b013e318255bb4a.
35. Sehi M, Grewal DS, Sheets CW, et al. Diagnostic ability of Fourier-domain vs time domain optical coherence tomography for glaucoma detection. Am J Ophthalmol 2009;148:597–605. DOI: 10.1016/j.ajo.2009.05.030
36. Budenz D, Michael A, Chang R, et al. Sensitivity and specificity of the stratus OCT for perimetric glaucoma. Ophthalmology 2005;112(1):3–9. DOI: 10.1016/j.ophtha.2004.06.039.
37. Bowd C, Zangwill LM, Berry CC, et al. Detecting early glaucoma by assessment of retinal nerve fiber layer thickness and visual function. Invest Ophthalmol Vis Sci 2001;42(9):1993–2003.
38. Hwang YH, Kim YY. Glaucoma diagnostic ability of quadrant and clock-hour neuroretinal rim assessment using cirrus HD optical coherence tomography. Invest Ophthalmol Vis Sci 2012;53(4):2226–2234. DOI: 10.1167/iovs.11-8689.
39. Leung CK, Ye C, Weinreb RN, et al. Retinal nerve fiber layer imaging with spectral-domain optical coherence tomography: a study on diagnostic agreement with Heidelberg retinal tomograph. Ophthalmology 2010;117(2):267–274. DOI: 10.1016/j.ophtha.2009.06.061.
40. Park SB, Sung KR, Kang SY, et al. Comparison of glaucoma diagnostic capabilities of cirrus HD and stratus optical coherence tomography. Arch Ophthalmol 2009;127(12):1603–1609. DOI: 10.1001/archophthalmol.2009.296.
41. Leite MT, Rao HL, Zangwill LM, et al. Comparison of the diagnostic accuracies of Spectralis, Cirrus and RTVue optical coherence tomography devices in glaucoma. Ophthalmology 2011;118(7):1334–1339. DOI: 10.1016/j.ophtha.2010.11.029.
42. Mwanza J-C, Oakley JD, Budenz DL, et al. Ability of the cirrus HD-OCT optic nerve head parameters to discriminate normal from glaucomatous eyes. Ophthalmology 2011;118(2):241–248. DOI: 10.1016/j.ophtha.2010.06.036.
43. Hood DC, Raza AS, de Moraes CGV, et al. Glaucomatous damage of the macula. Prog Retin Eye Res 2013;32:1e21. DOI: 10.1016/j.preteyeres.2012.08.003.
44. Pan Y, Varma R. Natural history of glaucoma. Indian J Ophthalmol 2011;59(suppl 1):S19–S23. DOI: 10.4103/0301-4738.73682.
45. Jonas JB, Born AM. Optic disc photography in the diagnosis of glaucoma. In: Shaarawy TM, et al. GLAUCOMA: Medical Diagnosis & Therapy. 2nd ed., London: Elsevier Saunders; 2015. 209–220.
46. Leung CKS, Choi N, Weinreb RN. Retinal nerve fiber layer imaging with spectral-domain optical coherence tomography: pattern of RNFL defects in glaucoma. Ophthalmology 2010;117(12):2337–2344. DOI: 10.1016/j.ophtha.2010.04.002.
47. Xu G, Weinreb RN, Leung CKS. Retinal nerve fiber layer progression in glaucoma a comparison between retinal nerve fiber layer thickness and retardance. Ophthalmology 2013;120(12):2493–2500. DOI: 10.1016/j.ophtha.2013.07.027.
48. Finzi A, Strobbe E, Tassi F, et al. Hemifield pattern electroretinogram in ocular hypertension: comparison with frequency doubling technology and optical coherence tomography to detect early optic neuropathy. Dovepress 2014;2014:1929–1936. DOI: 10.2147/OPTH.S67193.
49. Mwanza J, Durbin MK, Budenz DL. Interocular symmetry in peripapillary retinal nerve fiber layer thickness measured with the cirrus HD-OCT in healthy eyes. Am J Ophthalmol 2011;151(3):514–521. DOI: 10.1016/j.ajo.2010.09.015.
50. Ghadiali Q, Hood DC, Lee C, et al. An analysis of normal variations in retinal nerve fiber layer thickness profiles measured with optical coherence tomography. J Glaucoma 2008;17(5):333–340. DOI: 10.1097/IJG.0b013e3181650f8b.
51. Sullivan-Mee M, Ruegg CC, Pensyl D, et al. Diagnostic precision of retinal nerve fiber layer and macular thickness asymmetry parameters for Identifying early primary open-angle glaucoma. Am J Ophthalmol 2013;156(3):567–577. DOI: 10.1016/j.ajo.2013.04.037.
52. Park HYL, Shin HY, Yoon JY, et al. Intereye comparison of cirrus OCT in early glaucoma diagnosis and detecting photographic retinal nerve fiber layer abnormalities. Invest Ophthalmol Vis Sci 2015;56(3):1733–1742. DOI: 10.1167/iovs.14-15450.
53. Asrani S, Rosdahl JA, Allingham R. Novel software strategy for glaucoma diagnosis asymmetry analysis of retinal thickness. Arch Ophthalmol 2011;129(9):1205–1211. DOI: 10.1001/archophthalmol.2011.242.
54. Khanal S, Davey PG, Racette L, et al. Intraeye retinal nerve fiber layer and macular thickness asymmetry measurements for the discrimination of primary open-angle glaucoma and normal tension glaucoma. J Optom 2016;9(2):118–125. DOI: 10.1016/j.optom.2015.10.002.
55. Budenz DL. Symmetry between the right and left eyes of the normal retinal nerve fiber layer measured with optical coherence tomography (an AOS thesis). Trans Am Ophthalmol Soc 2008;106:252–275.
56. Badalà F, Nouri-Mahdavi K, Raoof DA, et al. Optic disc and nerve fiber layer imaging to detect glaucoma. Arch Ophthalmol 2007;144(5):724–732. DOI: 10.1016/j.ajo.2007.07.010.
57. Medeiros FA, Zangwill LM, Bowd C, et al. Evaluation of retinal nerve fiber layer, optic nerve head, and macular thickness measurements for glaucoma detection using optical coherence tomography. Am J Ophthalmol 2005;139(1):44–55. DOI: 10.1016/j.ajo.2004.08.069.
58. Pablo LE, Ferreras A, Pajarín AB, et al. Diagnostic ability of a linear discriminant function for optic nerve head parameters measured with optical coherence tomography for perimetric glaucoma. Eye 2010;24(6):1051–1057. DOI: 10.1038/eye.2009.245.
59. Sugimoto K, Murata H, Hirasawa H, et al. Cross-sectional study: Does combining optical coherence tomography measurements using the 'Random forest' decision tree classifier improve the prediction of the presence of perimetric deterioration in glaucoma suspects? Br J Ophthalmol 2013;3(10):e003114-1-7. DOI: 10.1136/bmjopen-2013-003114.
60. Mwanza JC, Warren JL, Budenz DL. Combining spectral domain optical coherence tomography structural parameters for the diagnosis of glaucoma with early visual field loss. Invest Ophthalmol Vis Sci 2013;54(13):8393–8400. DOI: 10.1167/iovs.13-12749.
61. Loewen NA, Zhang X, et al. Combining measurements from three anatomical areas for glaucoma diagnosis using Fourier-domain optical coherence tomography. Br J Ophthalmol 2015;99(9):1224–1229. DOI: 10.1136/bjophthalmol-2014-305907.
62. Choi YJ, Jeoung JW, Park KH, et al. Clinical use of an optical coherence tomography linear discriminant function for differentiating glaucoma from normal eyes. J Glaucoma 2016;25(3):e162–e169. DOI: 10.1097/IJG.0000000000000210.